The Journal of Experimental Biology 207, 767-776
Published by The Company of Biologists 2004
doi:10.1242/jeb.00817

A hierarchical analysis of the scaling of force and power production by dragonfly flight motors

Rudolf J. Schilder* and James H. Marden

208 Mueller Laboratory, Department of Biology, Pennsylvania State University, University Park, PA 16802, USA

*Author for correspondence (e-mail: rjs360@psu.edu)

Accepted 25 November 2003

Summary

Maximum isometric force output by single muscles has long been known to be proportional to muscle mass$^{0.67}$, i.e to muscle cross-sectional area. However, locomotion often requires a different muscle contraction regime than that used under isometric conditions. Moreover, lever mechanisms generally affect the force outputs of muscle–limb linkages, which is one reason why the scaling of net force output by intact musculoskeletal systems can differ from mass$^{0.67}$. Indeed, several studies have demonstrated that force output by intact musculoskeletal systems and non-biological systems is proportional to motor mass$^{1.0}$. Here we trace the mechanisms that cause dragonflies to achieve a change from muscle mass$^{0.67}$ scaling of maximum force output by single flight muscles to mass$^{1.0}$ scaling of dynamic force output by the intact dragonfly flight motor. In eight species of dragonflies, tetanic force output by the basalar muscle during isometric contraction scaled as muscle mass$^{0.67}$. Mean force output by the basalar muscle under dynamic conditions (workloops) that simulated *in vivo* maximum musculoskeletal performance was proportional to muscle mass$^{0.83}$, a significant increase in the scaling exponent over that of maximum isometric force output. The dynamic performance of the basalar muscle and the anatomy of its lever, consisting of the second moment of area of the forewing (d_2) and the distance between the muscle apodeme and the wing fulcrum (d_1), were used to analyze net force output by the integrated muscle-lever system (F_{ind}). The scaling of d_2 conformed closely to the expected value from geometic similarity (proportional to muscle mass$^{0.31}$), whereas d_1 scaled as muscle mass$^{0.54}$, a significant increase over the expected value from geometric similarity. F_{ind} scaled as muscle mass$^{1.036}$, and this scaling exponent was not significantly different from unity or from the scaling exponent relating maximum load-lifting by flying dragonflies to their thorax mass. Thus, the combined effect of a change in the scaling of force output by the muscle during dynamic contraction compared to that during isometric contraction *and* the departure from geometric similarity of one of the two lever arm lengths provides an explanation for how mass$^{1.0}$ scaling of force output by the intact musculoskeletal system is accomplished. We also show that maximum muscle mass-specific net work and power output available scale as mass$^{0.43}$ and mass$^{0.24}$, respectively.

Key words: force, work, power, scaling, allometry, dynamic force output, dragonfly, flight motor, lever arm, basalar muscle, work loop, load lifting.

Introduction

One of the most clearly established and widely known facts in locomotor physiology is that the maximum force exerted by a muscle is determined by its cross-sectional area, i.e. the number of actomyosin cross-bridges working in parallel (Hill, 1950). Because of this relationship and the general shape similarity of most muscles, muscle force output scales consistently as muscle mass$^{0.67}$. However, muscles rarely exert their forces directly on the external environment without some form of mechanical linkage in which lever arms and their associated mechanical advantage either enhance or reduce the forces generated by muscles (e.g. Biewener, 1989). Thus, force output by intact musculoskeletal systems can be quite different than that of individual muscles, and the scaling of this force output can differ markedly from mass$^{0.67}$.

Data from swimming fish (Webb, 1978), running and hopping animals (Full et al., 1991; Blob and Biewener, 2001; Biewener et al., 1988; Ritter et al., 2001) and flying animals (Marden, 1987) indicate that maximum force output of intact musculoskeletal systems scales very nearly as mass$^{1.0}$. More recently, Marden and Allen (2002) have shown that maximum force output by all types of rotary motors (musculoskeletal systems and man-made machines such as piston engines, jets, and electric motors that use rotary or oscillatory motion to accomplish more than simple translational motion of a load) scales as motor mass$^{1.0}$, and can be described by a single scaling equation in which the motor mass-specific force is 57±14 N kg^{-1} (mean ± S.D.).

The question of *why* different types of motors show such

similarity in both the magnitude and scaling of maximal force output is a complex question that is beyond the scope of this study. Here, we focus on *how* motor mass$^{1.0}$ scaling of force output by a biological motor is achieved by examining the morphology and mechanics of dragonfly musculoskeletal systems in a hierachical fashion, from the static force output of single muscles to the dynamic force output of the intact animal. Maximum force output by dragonfly flight muscle mass has previously be shown to scale isometrically with flight muscle mass (Marden, 1987). Our objective is to identify how an intact musculoskeletal system changes the scaling of force output from muscle mass$^{0.67}$ to muscle mass$^{1.0}$.

The dragonfly flight motor consists mainly of synchronous muscles that act directly on the wings. Up- and downstroke muscles insert on opposite sides of an internal pivot or fulcrum (Simmons, 1977). As such, the wings combined with fulcra, and either up- or downstroke muscles act as first and third order levers, respectively. We have chosen a downstroke muscle and its lever system as the focus of our analyses. All references to force output will refer to maximal force output, unless stated otherwise.

At least two potential mechanisms could account for the difference in scaling between isometric force output by individual muscles and dynamic force output by intact musculoskeletal systems. First, although maximum isometric force output of muscles scales as mass$^{0.67}$, dynamic force output by the muscle might scale with a higher exponent due to differences in mechanics of isometric *versus* dynamic oscillatory contraction. Small muscles tend to operate at higher contraction frequencies (Medler, 2002). At higher frequencies, transitions from an inactive (relaxation) to an active (contraction) state and *vice versa* will constitute a relatively greater portion of the total contraction cycle of the muscle, assuming that calcium release and uptake by the sarcoplasmic reticulum occurs at a rate that scales independently of mass. This would allow relatively less time for complete cross-bridge activation and relaxation and therefore a lower proportion of attached crossbridges during each cycle (i.e. Rome and Lindstedt, 1998; Rome et al., 1999). Dynamic force output by small muscles could therefore be relatively low compared to force output by larger muscles, and an increase in the scaling exponent that relates force output to muscle mass is expected.

Secondly, the scaling of force output of a musculoskeletal system is a function of the scaling of the dynamic force output and the geometry of lever arms present in the musculoskeletal system. Biewener (1989) showed that allometry of lever arms can compensate for unequal scaling of skeletal cross-sectional area and body mass in terrestrial vertebrates. Changes in limb posture (and associated changes in mechanical advantage) toward a more upright position of the supporting leg bones prevent large animals from operating at very low safety factors for stresses acting on the skeleton.

Departures from geometric similarity in mechanisms that affect force output need not be restricted to terrestrial vertebrate locomotion. Geometrical changes within musculoskeletal systems could compensate for the loss of force with increasing size (i.e. the mass$^{0.67}$ scaling of maximum force output) in order to achieve mass$^{1.0}$ scaling of dynamic force output by the intact musculoskeletal system.

We examine the possibility that dragonflies depart from geometrical similarity in the scaling of lever arm lengths within their thorax. Insect wing lengths have previously (Greenewalt, 1962, 1975) been shown to scale with mass$^{0.33}$, i.e. conform to geometric similarity (length$\propto$mass$^{0.33}$), but the scaling of internal lever arms used in insect thoracic musculoskeletal systems is unknown.

Our hierarchical approach started by measuring the maximum force output (F_{stat}) of the basalar muscle while it was held at constant length (i.e. an isometric contraction). We then determined mean force output generated by muscles during oscillatory contraction regimes (i.e. workloops; Josephson, 1985) that approximated *in vivo* working conditions during maximally loaded flight. This force output will be referred to as F_{dyn}.

Through its lever system, F_{dyn} produced by the muscle is utilized to satisfy inertial and aerodynamic force requirements, the latter of which can be further divided into induced, parasite and profile force requirements. The mean inertial and aerodynamic forces act at different distances along the wing. To make our analysis tractable, we chose a single external lever arm length (d_2), the distance along the wing at which the mean induced aerodynamic force acts (the radius of the second moment of wing area; Ellington 1984a).

We defined the internal lever arm length as the distance between the muscle apodeme and the forewing fulcrum (d_1). Then, assuming that moments are balanced about the wing fulcrum (Fig. 1), we calculated the induced force produced by

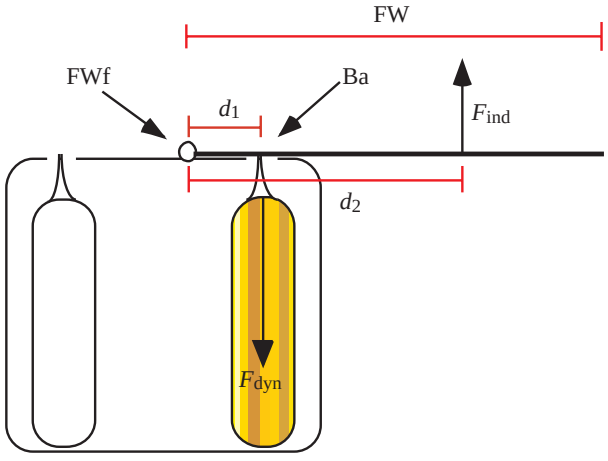

Fig. 1. Schematic representation of a basalar muscle and its third order lever system. FWf indicates the position of the wing fulcrum, FW represents forewing length and Ba indicates the position of the apodeme of the basalar muscle. The basalar muscle (yellow) produces force F_{dyn}, which is then transmitted through d_1, the distance between the basalar apodeme and wing fulcrum, and d_2, the second moment of wing area where the mean aerodynamic force acts.

this muscle-lever system (F_{ind}) during maximum performance conditions. Finally, we compared the scaling exponent of F_{ind} to that of the induced force output by the intact dragonfly thoracic musculature during maximum load lifting (F_{lift}).

In addition to analyzing the scaling of maximum force output by the musculoskeletal system, we present scaling relationships for both muscle mass-specific work and power output during maximum load lifting conditions.

Materials and methods

Animals

Adult male dragonflies (Odonata; Anisoptera) were collected with insect nets at several ponds in Centre County, Pennsylvania, USA. After capture, dragonflies were placed into plastic containers containing moistened paper towels and transported to the laboratory in a cooler. Containers were stored in a refrigerator at 4°C. Specimens were used in experiments within 12 h of capture. We used eight species in total, varying in mean body mass from 110 mg to 1.06 g (Table 1).

Muscle

We studied the performance of the basalar muscle of the mesothorax (terminology according to Marden et al., 2001), which functions as the main depressor of the leading edge of the forewing. It inserts directly on the humeral plate of the wing base by means of a tendinous connection to an apodeme (Snodgrass, 1935). The basalar muscle is not the only muscle that contributes to the depression of the forewing. The first subalar depressor assists the basalar in depression, and three smaller muscles (first basalar, second subalar depressor and third subalar depressor) are partly responsible for depression and supination of the wing (Simmons, 1977).

Load lifting experiments

In order to obtain F_{lift}, we incrementally increased a dragonfly's body mass and examined its capability to lift this additional mass (Marden, 1987). Lead weights were glued to the abdomen, after which the dragonfly was placed for approximately 1 min in an incubator set to 36°C to warm the flight muscles to an appropriately high temperature. Dragonflies were then placed on a white floor and stimulated to attempt take-off. They cooled quickly when removed from the incubator and were probably flying at a thoracic temperature of approximately 33–34°C. Added loads were increased until the specimen was just able to take off from the ground. Take-off attempts were recorded using a high-speed video camera (Redlake Imaging, San Diego, CA, USA) at 500 frames s^{-1} with the camera situated at an angle that allowed an approximate head-on view of the body axis. F_{lift} was calculated as maximum load lifted (body mass + added mass). Mean mass-specific F_{lift} was obtained by dividing F_{lift} by total thoracic muscle mass. Video records of flight attempts were analysed using iMovie© and NIH image© software. Wingbeat frequency and amplitude were calculated over three consecutive wingbeat cycles and were used with estimates of the internal lever arm length to calculate the basalar muscle length changes and muscle contraction frequencies during maximum load-lifting performance. These values were then used as input values for the workloop experiments.

Table 1. *Species used in this study and their body mass*

Family	Species	Body mass (g)	*N*
Aeshnidae	*Anax junius* (Drury)	1.06±0.12	10
	Aeshna umbrosa umbrosa (Walker)	0.62±0.06	3
Libellulidae	*Plathemis lydia* (Drury)	0.45±0.04	9
	Tramea lacerata (Hagen)	0.44±0.05	6
	Libellula luctuosa (Burmeister)	0.35±0.04	11
	Erythemis simplicicollis (Say)	0.23±0.03	8
	Sympetrum janae (Carle)	0.12±0.02	6
	Sympetrum vicinum (Hagen)	0.11±0.007	2

Values are means ± S.D. for *N* measurements.

Aeshna u. umbrosa specimens were not tested for their load lifting capability. Consequently, no dynamic force measurements (workloops) were performed on these specimens and no values for F_{ind} were obtained. Morphological data and F_{stat} measurements were obtained from *Aeshna u. umbrosa* specimens, as these data did not depend on input values obtained from load lifting experiments.

Mechanical isolation of the basalar muscle

Dragonflies were decapitated and their legs and wings clipped. The abdomen was left intact so that it continued to rythmically ventilate the thorax. Using an epoxy resin, thoraces with the abdomen still attached were glued into a temperature-controlled aluminum test chamber. The thorax was set into a position in which the basalar muscle fibres were running vertically. In order to keep the surrounding air moist and prevent dessication, a wetted tissue was placed within the chamber. The cuticle surrounding the basalar muscle apodeme was cut free, thus mechanically isolating the basalar muscle from the rest of the thorax. A fine suture was tied around the apodeme and glued to a modified insect pin suspended from the lever arm of a lever system (Cambridge Technology 300B, Cambridge, MA, USA). Before the onset of F_{stat} measurements and workloop experiments, a micromanipulator controlling the position of the lever arm was used to carefully stretch the basalar muscle to its original position, which was determined by comparing it to the position of the neighbouring muscles and wingbase.

Isometric tetanus experiments

The stimulation frequency used to produce F_{stat} was 285 Hz, which yielded maximum static tension for all species in preliminary experiments. An S48 stimulator (Grass Instruments, Quincy, MA, USA) produced trains of 0.25 ms pulses to the basalar muscle through two fine-gauge electrodes inserted on each side of the mesothorax. The intensity of the

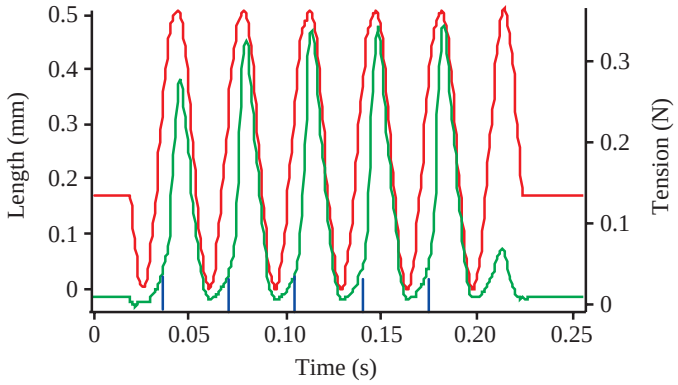

Fig. 2. Example of raw data obtained during a workloop experiment. The sinusoidal length cycles are shown in red, the timing of stimulation is shown in blue, and resulting tension developed by the basalar muscle is shown in green. Tension data from the fourth cycle were used for further analyses.

stimuli was set to a level that produced maximal twitch tension; this level was generally about 1.0 V. The maximum force produced during a period of 0.5 s of complete tetanus was recorded. Isometric tetanus experiments were performed approximately 10 min after workloop experiments (see below); we chose this order of experiments because our muscle preparations frequently performed poorly after being subjected to isometric tetanus.

Workloop experiments

The basalar muscle was driven through a series of five sinusoidal length cycles (Fig. 2). For each species, the amount of imposed length change during these cycles was calculated using species-specific lever arm length measurements and the wingbeat amplitudes obtained from the load-lifting experiments. Similarly, the muscle contraction frequency used for workloop analyses was the mean wingbeat frequency used by that species during maximum load lifting. The phase relationship between electrical stimulation and muscle strain was set at a value previously determined to be the *in vivo* phase relationship for basalar activation in one species of dragonfly (activation at 44% of maximum length during the lengthening phase; Marden et al., 2001). Net work produced by the basalar muscle was measured from the workloop area during the fourth length cycle. Mean force produced during a length cycle (F_{dyn}) was calculated as net work produced divided by the muscle strain during the loop.

Stimulation magnitude and duration settings were identical to those described above for the isometric force measurements. Thoracic temperature was monitored using a fine-gauge thermocouple that was inserted into the metathorax and connected to a TC-1000 thermometer (Sable Systems, Las Vegas, NV, USA). Thoracic temperature during workloop experiments was regulated between 32–34°C.

Anatomical measurements

Total thorax and basalar muscle wet mass of dragonflies were measured to the nearest 0.1 mg using an analytical balance. The non-dimensional radius of the second moment of forewing area was calculated according to Ellington (1984a) and multiplied by forewing length in order to obtain d_2. To measure d_1, the internal lever arm length, a section of the dorsal thorax containing a forewing fulcrum and basalar apodeme was cut out of the thorax, after which all muscle and soft tissue except for the apodeme of the basalar muscle was removed (Fig. 3). Micrographs were taken using a DC200 digital camera (Leica, Cambridge, UK) attached to a Leica MZ 125 microscope and analysed using NIH image© software.

Calculation of motor force output

F_{ind} was calculated according to the following equation for balanced moments over the wing fulcrum, using measured values of F_{dyn}, d_1 and d_2 for each individual:

$$F_{dyn}d_1 = F_{ind}d_2 \,. \quad (1)$$

This use of the lever model neglects the fact that the effective lever arm lengths change as a result of the changing wing position during a wingstroke. However, both effective d_1 and d_2 values will always change to the same extent, because effective lever arms during a wingstroke are equal to cosα×lever arm length, where α is the wing angle, hence not changing the ratio of the two used to calculate F_{ind}.

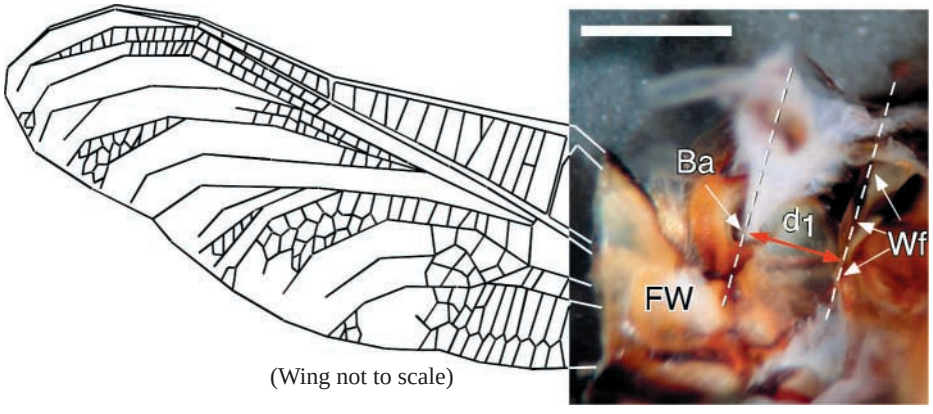

Fig. 3. Detailed ventral view of the internal surface of the *Anax junius* dorsal thorax at the base of the forewing, showing the location of the basalar muscle apodeme (Ba) and the wing fulcrum (Wf) of the forewing (FW). The distance between these two structures is the muscle apodeme-to-wing fulcrum lever arm length (d_1). All muscle tissue has been removed. Scale bar, 1 mm. A portion of the wing is drawn to orient the reader; this wing is not to scale.

Scaling and statistical analyses

The scaling analyses performed on the variables d_1, d_2, F_{dyn} and F_{ind} were done with respect to the wet mass of the basalar muscle. For F_{lift}, total thoracic muscle mass was used. Data were log-transformed and each of the variables measured were fitted using a least-squares linear regression model. The scaling exponent for F_{ind} was obtained by first calculating values for F_{ind} according to Equation 1, after which calculated F_{ind} values were regressed with respect to muscle mass. Scaling exponents were tested against hypothesized exponents using *t*-tests (Draper and Smith, 1981; Zar, 1984). Statistical analyses were conducted using JMP software (SAS Institute Inc., Cary, NC, USA).

Results

Maximum force output by intact flight motors

Maximum force output by intact flight motors (F_{lift}) produced by a range of species was proportional to thorax muscle mass$^{1.035}$ (Fig. 4A). A two-tailed *t*-test showed that this scaling exponent did not differ statistically from 1.0 (α=0.05, P=0.338, N=10). This result agrees with earlier findings for flying insects (Marden, 1987) and for a large sample and variety of animate and inanimate motors (Marden and Allen, 2002). Mean mass-specific F_{lift} was 40.0±3.0 N kg^{-1} (mean ± S.D.).

Isometric force output

Isometric force output (F_{stat}) was proportional to muscle mass$^{0.670}$ (Fig. 4B). A two-tailed *t*-test confirmed that the scaling exponent was not statistically different (α=0.05, P=0.948, N=10) from 0.667, indicating that dragonfly basalar muscles behave similarly to most other muscles, i.e. maximum isometric force production is proportional to cross-sectional area.

Lever arms

Lever arm d_2 for this group of dragonflies was proportional to muscle mass$^{0.31}$ (Fig. 5A). A two-tailed *t*-test could not distinguish the d_2 scaling exponent from 0.33, the expected scaling of length with mass for similarly shaped bodies (α=0.05, P=0.173, N=51). In contrast, lever arm d_1 did not

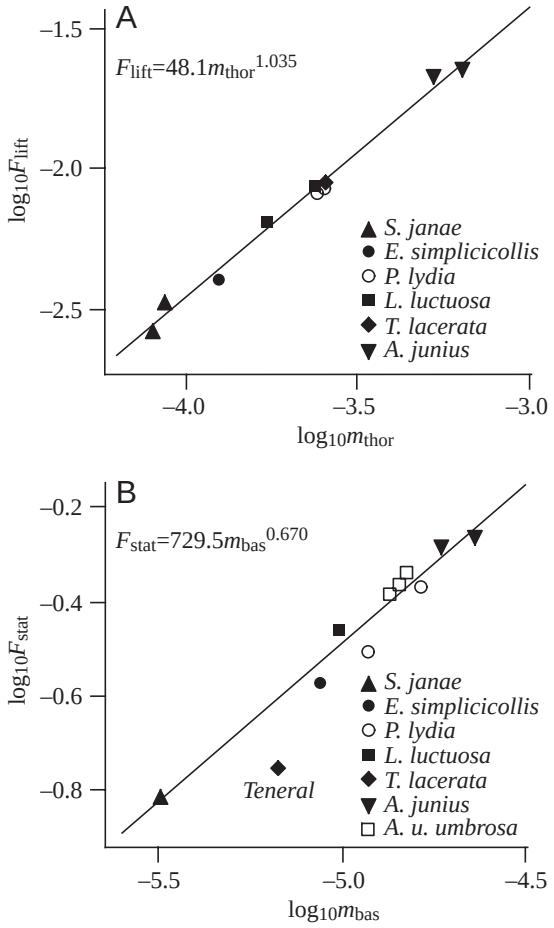

Fig. 4. (A) Maximum lifting force (F_{lift}) as a function of thorax mass (m_{thor}). $\log_{10}F_{lift}=1.682+1.035\log_{10}m_{thor}$ (r^2=0.99; S.E.$_{slope}$=0.036; N=10). (B) Maximum isometric force (F_{stat}) as a function of basalar muscle mass (m_{bas}). $\log_{10}F_{stat}=2.863+0.670\log_{10}m_{bas}$ (r^2=0.96; S.E.$_{slope}$=0.050; N=10). The datapoint marked '*Teneral*' indicates a newly emerged and therefore physiologically immature *T. lacerata*. This point was excluded from the regression analysis.

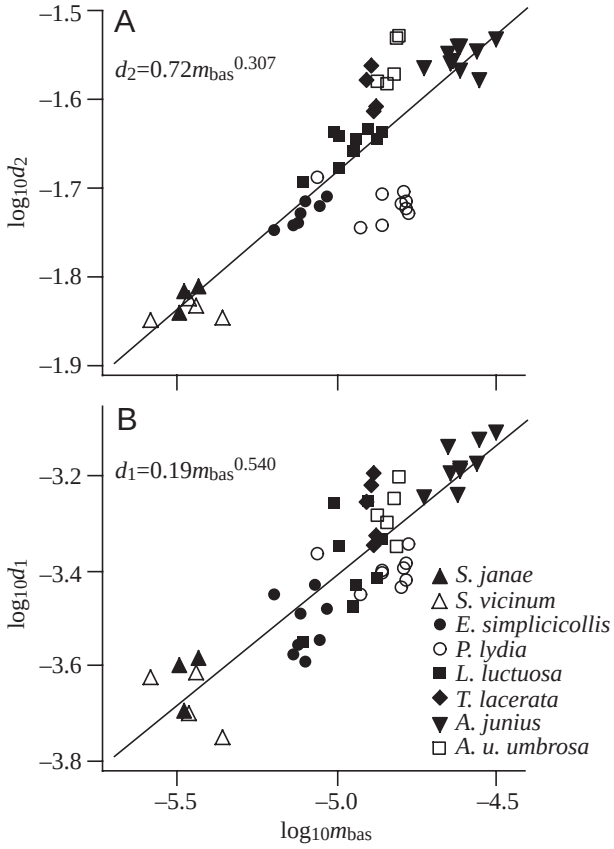

Fig. 5. (A) Effective lever arm length (d_2) as a function of basalar muscle mass (m_{bas}). $\log_{10}d_2=-0.143+0.307\log_{10}m_{bas}$ (r^2=0.72; S.E.$_{slope}$=0.027; N=51). Symbols are as in B. (B) Internal lever arm length (d_1) as a function of m_{bas}. $\log_{10}d_1=-0.710+0.540\log_{10}m_{bas}$ (r^2=0.77; S.E.$_{slope}$=0.042; N=52).

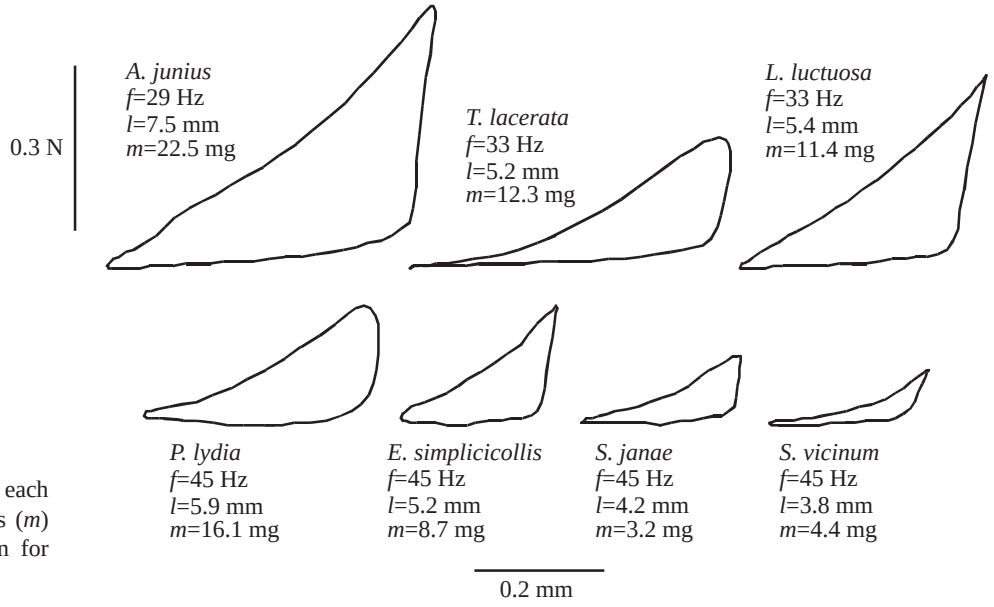

Fig. 6. Examples of workloops for each species. Basalar muscle length (*l*), mass (*m*) and contraction frequency (*f*) are given for each specimen.

scale according to the expectations of geometrical similarity, as d_1 was proportional to muscle mass$^{0.540}$ (Fig. 5B). This scaling exponent was significantly higher than the expected value of 0.33 (two-tailed *t*-test; α=0.05, P<<0.001, N=52).

Dynamic muscle force output

Fig. 6 shows examples of typical workloops for each species used in this study. Mean dynamic muscle force output during workloops (F_{dyn}) was proportional to muscle mass$^{0.83}$ (Fig. 7A). A one-tailed *t*-test indicated that this scaling exponent was significantly higher than 0.667 (α=0.05, P=0.029, N=33), but significantly lower than 1.0 (one-tailed t-test; α=0.05, P=0.027, N=33). This result shows that during realistic dynamic contraction, the scaling of muscle force output was different from that during static isometric conditions (F_{stat}) and from the scaling of intact flight motor force output (F_{lift}).

Muscle-lever system force output

The calculated force output (F_{ind}) produced by the muscle-lever system during maximum performance scaled as muscle mass$^{1.04}$ (Fig. 7B). This scaling exponent was not statistically different from 1.0 (two-tailed *t*-test; α=0.05, P=0.670, N=33) or from the scaling exponent (1.035) that we found for F_{lift} production by intact dragonflies (two-tailed *t*-test; α=0.05, P=0.982, N=33). Mean muscle mass-specific F_{ind} was 138.3±38.2 N kg^{-1} (mean ± S.D.).

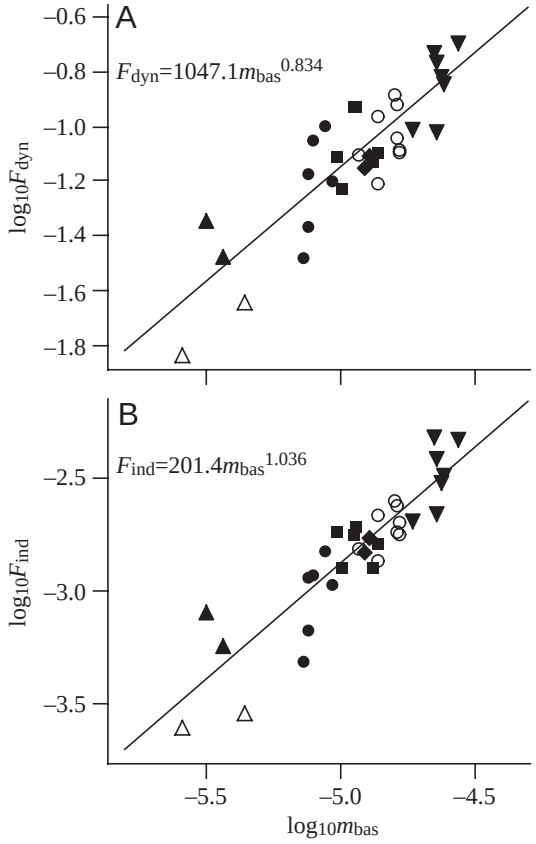

Fig. 7. (A) Mean dynamic force output (F_{dyn}) as a function of basalar muscle mass (m_{bas}). log$_{10}F_{dyn}$=3.020+0.834log$_{10}m_{bas}$ (r^2=0.76; S.E.$_{slope}$=0.086; N=33). (B) Force output during one maximal-effort muscle contraction cycle at the output end of the lever system (F_{ind}) as a function of m_{bas}. log$_{10}$ F_{ind}=2.304+1.036log$_{10}m_{bas}$ (r^2=0.83; S.E.$_{slope}$=0.086; N=33). Symbols are as in Fig. 5B.

Discussion

Scaling of maximum force output

The aim of this study was to determine how animal musculoskeletal systems achieve mass$^{1.0}$ scaling of maximum induced force production (Marden, 1987; Marden and Allen, 2002). To do this, we studied the performance and design of a

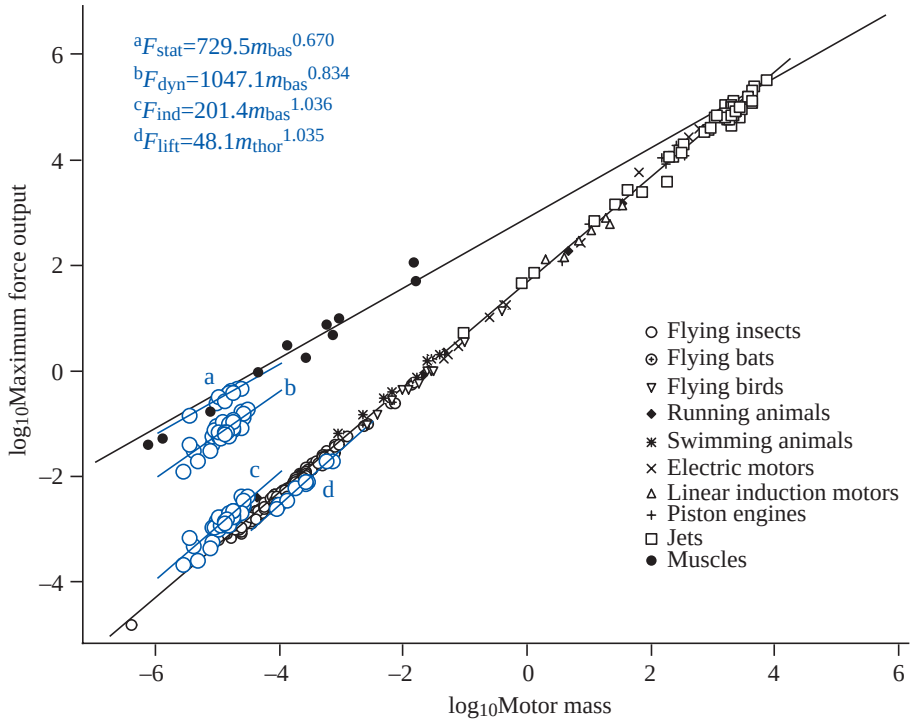

Fig. 8. Maximum force output as a function of motor mass for 'Group 2 motors' and single muscles (Marden and Allen, 2002). The upper and lower (grey) linear regression equations are $\log_{10}$Max. force output=2.95+0.667$\log_{10}$Muscle mass and $\log_{10}$Max. force output= 1.74+0.999$\log_{10}$Motor mass, respectively. Blue graphs a, b, c and d represent data and scaling equations obtained in this study. 'Motor mass' is synonymous to thorax mass (m_{thor}) for F_{lift} data. Basalar muscle mass (m_{bas}) is used for F_{stat}, F_{dyn} and F_{ind} data.

dragonfly musculoskeletal system and determined how the scaling of force output varies across levels of biological organization.

Like other animal muscles, dragonfly basalar muscles held at constant length produce maximum forces that are proportional to muscle mass$^{0.67}$ (Fig. 8). However, the average force produced by the basalar muscle during realistic dynamic working conditions (i.e. during workloops) is proportional to muscle mass$^{0.83}$ (Fig. 8), a significant increase from the scaling of muscle force during isometric tetanus. The difference in scaling between isometric and dynamic force production is by itself insufficient to explain the mass$^{1.0}$ scaling of maximum force production by an intact dragonfly flight musculoskeletal system, since the scaling exponent 0.83 was significantly lower than 1.0.

Our data show that there is a departure from geometrical similarity in one of the lever arms within the musculoskeletal system, as d_1 scaled as muscle mass$^{0.54}$. This departure was specific to the small internal lever arm because d_2, the larger external lever arm, scaled as muscle mass$^{0.31}$, which was not significantly different from mass$^{0.33}$. The departure from geometric similarity for d_1 indicates allometry for a skeletal element rather than adjustments in posture or alignment of motor parts as has been reported for terrestrial mammals (Biewener, 1989). It is the combination of the allometry of d_1 and the scaling of F_{dyn} that causes the scaling of F_{ind} to be very close to muscle mass$^{1.0}$ (Fig. 8).

It should be noted that the particular combination of scaling parameters for dragonfly flight musculoskeletal systems is probably idiosyncratic to this system and that other combinations of scaling relationships could also result in mass$^{1.0}$ scaling of force output. If dynamic force output in another system should scale with an exponent other than 0.83, then we expect a compensating difference in the scaling of at least one of the lever arms, in order to maintain mass$^{1.0}$ scaling of total system force output. It remains to be seen how general the value of 0.83 is for F_{dyn} in other taxa, but if differences between the scaling of isometric and dynamic force output are common, then scaling models that assume a value of 0.67 (e.g. Wakeling et al., 1999; Hutchinson and Garcia, 2000) should be used with caution.

Our analyses treated all data points as independent; however, the phylogenetic relatedness within and between species makes this assumption worth examining (Pagel and Harvey, 1988; Felsenstein, 1985). We repeated the regression analyses using mean values calculated for each species. No substantial change in the scaling exponents was detected [for example, the scaling exponent for F_{ind} became 1.058 for species means (N=8) instead of 1.036 for all individuals], indicating that the use of individual datapoints in the regression analyses did not bias our results. Similarly, when the data set was collapsed to mean values for genera (N=7) or family (N=2) there was no substantial change in the estimated scaling exponent of F_{ind} (Table 2 shows a full list of scaling exponents for d_1, d_2, F_{dyn} and F_{ind} generated by these different analyses).

Our focus in this study was to examine the scaling of force output; however, it is also interesting to compare the magnitude of the forces we measured and calculated with measures from previous studies. Although the scaling exponent for maximum load lifting force output agrees with the scaling slopes found by a previous survey of load lifting by flying animals (Marden, 1987) and a broader survey of net force output by nearly all types of motors used for animal and mechanized transportation (Fig. 8; Marden and Allen, 2002),

our measure of mean mass-specific F_{lift} is low compared to the mean mass-specific maximum force output (57±14 N kg^{-1}) found in those studies. In our calculations of F_{lift}, we used the maximum weight carried by dragonflies, whereas previous studies used the midway point between the maximum weight carried and the next incremental load that could not be carried (Marden, 1987). This difference is at least partly responsible for the somewhat lower mean mass-specific F_{lift} data presented in this study.

Our loaded dragonflies flew forward at velocities between 1 and 1.8 m s^{-1}. This implies that whole motor force output is higher than the maximum weight carried, by an amount equal to the force necessary to overcome parasite drag and profile drag at such speed. We used published values for mean parasite and profile drag forces on *Sympetrum sanguineum* dragonflies that were gliding at 2 m s^{-1} (Wakeling and Ellington, 1997a) to estimate this additional force. The adjusted force output was not substantially different from the value for mass-specific F_{lift} (40.2 N kg^{-1} instead of 40 N kg^{-1}), indicating that average parasite and profile force requirements at these low speeds are negligible in comparison with induced force requirements. However, wing kinematics are different during maximum load lifting compared to those during free gliding flight, and mean parasite and profile drag values could therefore be different.

Table 2. *Terms of fit for the least-squares linear regression of mean log$_{10}$-transformed values of* d_1, d_2, F_{dyn} *and* F_{ind} *for data sets containing values for individuals or mean values for species, genera and family*

	Data set			
Variable	Individuals	Species	Genera	Family
d_1				
Slope	0.54	0.55	0.57	0.65
S.E.	0.04	0.07	0.08	–
Intercept	–0.71	–0.64	–0.56	–0.17
r^2	0.77	0.92	0.90	–
N	52	8	7	2
d_2				
Slope	0.31	0.34	0.34	0.42
S.E.	0.03	0.06	0.08	–
Intercept	–0.14	0.002	0.008	–0.17
r^2	0.72	0.83	0.77	–
N	51	8	7	2
F_{dyn}				
Slope	0.83	0.86	0.84	0.84
S.E.	0.09	0.15	0.09	–
Intercept	3.02	3.16	3.05	3.05
r^2	0.76	0.88	0.96	–
N	32	7	6	2
F_{ind}				
Slope	1.04	1.06	1.05	1.08
S.E.	0.09	0.16	0.03	–
Intercept	2.30	2.41	2.39	2.50
r^2	0.83	0.90	0.99	–
N	32	7	6	2

S.E. is the standard error of the least-squares regression slope; N is the sample size for each of the variables.

For definitions of d_1, d_2, F_{dyn} and F_{ind}, see List of symbols.

Mean mass-specific F_{ind} was calculated to be 138.3 N kg^{-1}, which is higher than the mean value for F_{lift} for loaded dragonflies and the mass-specific force output by motors in general (Marden and Allen, 2002). At least part of this difference is due to the fact our calculated value for F_{ind} assumes that all of the force output is used to create induced lift. However, this simplification ignores the fact that force output by the flight motor must also meet inertial, parasite and profile force requirements.

Inertial force requirements especially are known to be substantial during dragonfly flight. Work needed to accelerate wings and virtual masses during hovering flight can be between 1.4 and 5.9 times the work done against aerodynamic forces (Ellington, 1984b). During forward flight, however, inertial force requirements have been shown to be lower than aerodynamic requirements (Wakeling and Ellington, 1997b). Although we did not measure inertial requirements quantitatively in this study, they are particularly interesting with regard to the results of our scaling analysis. If we assume that average parasite and profile force requirements are negligible (see above), then the total moment required from the muscle and lever arms can be described as:

$$M_{total} = (F_{ind}d_2) + (F_{inertial}d_3)\ , \quad (2)$$

where M_{total} is the product of F_{dyn} and the internal lever arm d_1, and d_3 is the effective lever arm length through which $F_{inertial}$ acts, i.e. the centre of forewing mass (Ellington, 1984a). Previously published equations for the radii of moments of wing mass and wing area (equations 23 and 29 in Ellington, 1984a) were used to calculate values for d_3. The muscle mass-specific scaling exponent of d_3 was found to be the same as that of d_2, i.e. scaling as muscle mass$^{0.31}$. Because the scaling exponent of M_{total} is approximately 1.35, and the two external lever arm lengths for the mean distance of action of induced and inertial forces both scale as mass$^{0.31}$, it follows that the sum of F_{ind} and $F_{inertial}$ must scale as approximately mass$^{1.04}$. Induced force output should scale with the same exponent as does load lifting ability (mass$^{1.035}$), and therefore inertial force requirements must scale also as approximately mass$^{1.0}$.

This study demonstrates a mechanism by which dragonflies achieve the 'universal' mass$^{1.0}$ scaling of maximum force output, but it cannot explain *why* this is true for most types of biological and engineered motors. Marden and Allen (2002) have discussed the idea that mass$^{1.0}$ scaling of force output and the universal upper limit of mass-specific force output by rotational motors represents a failure mode above which there may be a drop-off in durability. Perhaps complex stress regimes (Marden and Allen, 2002) require a motor to have a constant ratio of mass to net force output in order to be durable and successful. This remains a highly speculative idea, but no other hypotheses have been put

forward to explain the universal mass$^{1.0}$ scaling of force output by rotational motors.

Scaling of muscle mass-specific work and power

Ellington (1991) used previously published data (Marden, 1987) to estimate that mass-specific muscle power output available during maximally loaded flight scales as mass$^{0.13}$ for flying animals spanning 19 mg to 920 g body mass. By assuming that wingbeat frequency scales as mass$^{-0.33}$, muscle mass-specific work was estimated to be proportional to mass$^{0.46}$. For Anisoptera within that sample, mass-specific muscle power was estimated to scale as mass$^{0.27}$, which implies a mass scaling exponent of approximately 0.60. In contrast to these results, Tobalske and Dial (2000) proposed that maximum mass-specific work by muscles could be invariant with size (i.e. scaling as mass^{0}) for Phasianidae, as they showed that pectoralis mass-specific take-off power in this group scaled approximately as mass$^{-0.33}$, i.e. maximum mass-specific power available was proportional to wingbeat frequency. However, take-off power analysed by the latter study represented an unknown fraction of the power available from the muscles and the scaling of total mechanical power output by Phasianid muscles during maximum performance could be different from mass$^{-0.33}$. Askew et al. (2001) reported a lower scaling exponent for mass-specific muscle power (i.e. mass$^{-0.14}$) available from Phasianid flight muscles, but the allometric scaling of wing beat frequency (i.e. mass$^{-0.247}$ scaling instead of the predicted mass$^{-0.33}$ scaling) found for this group indicated that mass-specific muscle work would indeed be largely independent of body mass. However, the inclusion of previously published data for hummingbirds, Harris' hawk and bees changed the scaling relationship of mass-specific work to mass$^{0.336}$. So, while mass-specific force output by different sized flight motors shows remarkable consistency in its scaling with mass (e.g. Marden, 1987; this study), it seems that the scaling of other important indicators of flight performance, muscle mass-specific work and power, shows more variation amongst different taxonomic groups.

Mass-specific power available from dragonfly basalar muscles during maximum performance (calculated using muscle work during strain regimes and contraction frequencies that matched maximally loaded flight) increased significantly with increasing body mass and was proportional to muscle mass$^{0.24}$ (Fig. 9A). Mass-specific work during maximum performance was proportional to muscle mass$^{0.43}$ (Fig. 9B), while wingbeat frequency scaled as mass$^{-0.20}$. Both of these values are in rough agreement with estimates by Ellington (1991) for Anisoptera, and provide some of the first directly measured data concerning the scaling of mass-specific work and power available from insect flight muscles during maximum performance.

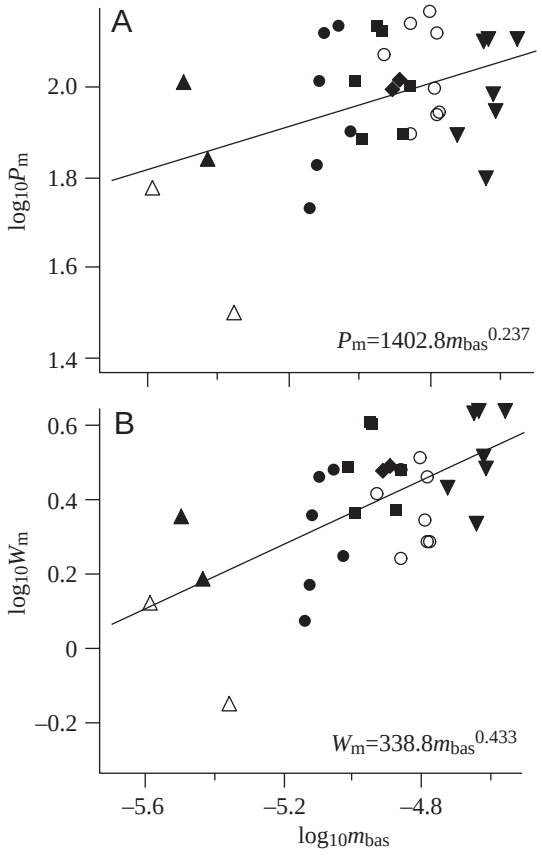

Fig. 9. (A) Mass-specific power (P_m) as a function of basalar mass (m_{bas}). $\log_{10}P_m$=3.147+0.237$\log_{10}m_{bas}$ (r^2=0.18; S.E.$_{slope}$=0.09; N=33). (B) Mass-specific work (W_m) as a function of m_{bas}. $\log_{10}W_m$=2.530+0.433$\log_{10}m_{bas}$ (r^2=0.39; S.E.$_{slope}$=0.10; N=33). Symbols are as in Fig. 5B.

List of symbols

d_1	distance between the muscle apodeme and the wing fulcrum
d_2	second moment of area of the forewing
d_3	centre of forewing mass
f	muscle contraction frequency
F_{dyn}	mean force output generated by muscles
F_{ind}	net force output by the integrated muscle-lever system
$F_{inertial}$	inertial force acting through d_3
F_{lift}	induced force output during maximum load lifting
F_{stat}	isometric force
l	muscle length
m	muscle mass
m_{bas}	basalar muscle mass
m_{thor}	thorax mass
M_{total}	product of F_{dyn} and arm d_1
P_m	mass-specific power
α	wing angle
W_m	mass-specific work

We thank Dr A. A. Biewener and two anonymous referees; their constructive criticisms greatly improved the manuscript. This material is based upon work supported by the National Science Foundation under Grant No. 0091040.

References

Askew, G. N., Marsh, R. L. and Ellington, C. P. (2001). The mechanical power output of the flight muscles of blue-breasted quail (*Coturnix chinensis*) during take-off. *J. Exp. Biol.* **204**, 3601-3619.

Biewener, A. A., Blickhan, R., Perry, A. K., Heglund, N. C. and Taylor, C. R. (1988). Muscle forces during locomotion in kangaroo rats: force platform and tendon buckle measurements compared. *J. Exp. Biol.* **137**, 191-205.

Biewener, A. A. (1989). Scaling body support in mammals: Limb posture and muscle mechanics. *Science* **245**, 45-48.

Blob, R. W. and Biewener, A. A. (2001). Mechanics of limb bone loading during terrestrial locomotion in the green iguana (*Iguana iguana*) and american alligator (*Alligator mississippiensis*). *J. Exp. Biol.* **204**, 1099-1122.

Draper, N. R. and Smith, H. (1981). *Applied Regression Analysis*. New York: John Wiley & Sons, Inc.

Ellington, C. P. (1984a). The aerodynamics of hovering insect flight. II. Morphological parameters. *Phil. Trans. R. Soc. Lond. B* **305**, 17-40.

Ellington, C. P. (1984b). The aerodynamics of hovering insect flight. VI. Lift and power requirements. *Phil. Trans. R. Soc. Lond. B* **305**, 145-181.

Ellington, C. P. (1991). Limitations on animal flight performance. *J. Exp. Biol.* **160**, 71-91.

Felsenstein, J. (1985). Phylogenies and the comparative method. *Am. Nat.* **125**, 1-15.

Full, R. J., Blickhan, R. and Ting, L. H. (2001). Leg design in hexapedal runners. *J. Exp. Biol.* **158**, 369-390.

Greenewalt, C. H. (1962). Dimensional relationships for flying animals. *Smithson. Misc. Collns* **144**, 1-46.

Greenewalt, C. H. (1975). The flight of birds. *Trans. Am. Phil. Soc. (New Ser.)* **65**, 1-67.

Hill, A. V. (1950). The dimensions of animals and their muscular dynamics. *Sci. Progr.* **38**, 209-230.

Hutchinson, J. R. and Garcia, M. (2002). *Tyrrannosaurus* was not a fast runner. *Nature* **415**, 1018-1021.

Josephson, R. K. (1985). Mechanical power output from striated muscle during cyclic contraction. *J. Exp. Biol.* **114**, 493-512.

Marden, J. H. (1987). Maximum lift production during takeoff in flying animals. *J. Exp. Biol.* **130**, 235-258

Marden, J. H. and Allen, L. R. (2002). Molecules, muscles, and machines: Universal performance characteristics of motors. *Proc. Natl. Acad. Sci. USA* **99**, 4161-4166.

Marden, J. H., Fitzhugh, G. H., Girgenrath, M., Wolf, M. R. and Girgenrath, S. (2001). Alternative splicing, muscle contraction and intraspecific variation: associations between troponin T transcripts, Ca^{2+} sensitivity and the force and power output of dragonfly flight muscles during oscillatory contraction. *J. Exp. Biol.* **204**, 3457-3470.

Medler, S. (2002). Comparative trends in shortening velocity and force production in skeletal muscles. *Am. J. Physiol. Reg. Int. Comp. Physiol.* **283**, R368-R378.

Pagel, M. D. and Harvey, P. H. (1988). Recent developments in the analysis of comparative data. *Q. Rev. Biol.* **63**, 413-440.

Ritter, D. A., Nassar, P. N., Fife, M. and Carrier, D. R. (2001). Epaxial muscle function in trotting dogs. *J. Exp. Biol.* **204**, 3053-3064.

Rome, L. C. and Lindstedt, S. L. (1998). The quest for speed: muscles built for high-frequency contractions. *News Physiol. Sci.* **13**, 261-268.

Rome, L. C., Cook, C., Syme, D. A., Connaughton, M. A., Ashley-Ross, M., Klimov, A., Tikunov, B. and Goldman, Y. E. (1999). Trading force for speed: Why superfast crossbridge kinetics leads to superlow forces. *Proc. Natl. Acad. Sci. USA* **96**, 5826-5831.

Simmons, P. (1977). The neuronal control of dragonfly flight. I. Anatomy. *J. Exp. Biol.* **71**, 123-140.

Snodgrass, R. E. (1935). *Principles of Insect Morphology*. New York: MacGraw-Hill.

Tobalske, B. W. and Dial, K. P. (2000). Effects of body size on take-off flight performance in the Phasianidae (Aves). *J. Exp. Biol.* **203**, 3319-3332.

Wakeling, J. M. and Ellington, C. P. (1997a). Dragonfly flight. I. Gliding flight and steady-state aerodynamic forces. *J. Exp. Biol.* **200**, 543-556.

Wakeling, J. M. and Ellington, C. P. (1997b). Dragonfly flight. III. Lift and power requirements. *J. Exp. Biol.* **200**, 583-600.

Wakeling, J. M., Kemp, K. M. and Johnston, I. A. (1999). The biomechanics of fast-starts during ontogeny in the common carp (*Cyprinus carpio*). *J. Exp. Biol.* **202**, 3057-3067.

Webb, P. W. (1978). Fast-start performance and body form in seven species of teleost fish. *J. Exp. Biol.* **74**, 211-226.

Zar, J. H. (1984). *Biostatistical Analysis.* New Jersey: Prentice-Hall, Inc.